Design of a Microcombustion-Based Heat Source for Thermoelectric Generation

Undergraduate Honors Thesis

Presented in Partial Fulfillment of the Requirements for

Graduation with Distinction

at The Ohio State University

By

Christine Orovets

* * * * *

The Ohio State University

2010

Defense Committee:

Professor Joseph Heremans, Advisor

Professor Shaurya Prakash, Advisor

Professor Yann Guezennec

ABSTRACT

Combustion processes are a series of chemical reactions between a fuel and an oxidant that produce heat at enormous energy density per unit weight of fuel consumed (40-50 MJ/kg). Thermoelectric generation is the direct conversion of heat to electricity. Thermoelectric devices are useful because there are no moving parts, and thus have long lifespans. The goal of this project was to use the heat from the combustion process in a millimeter scale combustor for thermoelectric generation in portable energy systems. The radial design with concentric spirals allows a heat-exchanger type configuration that permits a balance between heat conducted by the thermoelectric elements and convection between the gas streams due to the radial temperature gradient. The goal is for each unit to produce approximately 75 mV with Iron and Constantan thermoelectric metals integrated with an alumina microcombustor. The combustors are prepared by a multi-step fabrication process that begins with soft lithography of poly(dimethylsiloxane) or PDMS to generate a mold, followed by gel-casting of the alumina slurry in the mold to create a green body. This green body is then sintered in a high temperature furnace to yield a high density ceramic structure. Combustors have been fabricated, though some warping of the material occurs during the sintering. Research efforts focused on optimizing the fabrication procedure for repeatable construction of the combustors. First, a thermocouple was integrated with a simple microcombustor to produce a maximum voltage of 10.60 mV. In the next stage, the integration of the thermoelectric elements with the spiral geometry combustor was evaluated, though the radial gradient was not produced as expected. A maximum voltage of 1.06 mV was obtained. With less warping of the combustor during drying as well as more efficient sealing of the channel walls, this system could be capable of providing a high density power source by conversion of the high energy density of conventional fuel source for portable energy needs.

ACKNOWLEDGEMENTS

I would like to thank Dr. Shaurya Prakash and Dr. Joseph Heremans for their advising on this project. I would also like to thank Mary Hartzler and Neil Gardner for their help machining here at OSU, as well as Dr. Sudarsanam Babu and Jay Eastman for assisting me at the Edison Welding Institute.

TABLE OF CONTENTS

LIST OF FIGURES

LIST OF TABLES

CHAPTER 1: INTRODUCTION

The overall goal of this research is to design and fabricate a microcombustor with an integrated thermoelectric converter. The heat generated by the combustion is expected to create a temperature gradient that is converted to electricity. A voltage of approximately 75 mV should be produced with one 2.25" square device. A future goal is to stack 20 of these devices to create a 1.5V battery, the same voltage of a C-cell battery but with higher energy density.

Shown below is the basic concept for this design. This integrated TE-combustor is a heat source, counterflow heat exchanger, and TE power generator. The radial design that allows for a conduction-convection balance makes it possible to optimize the power of the TE material.

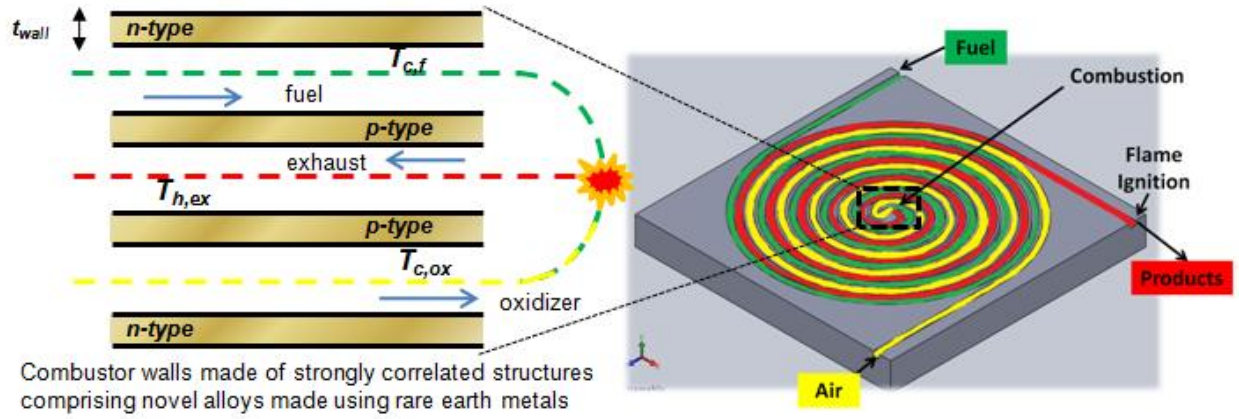

Figure 1: Concept of integrated TE-microcombustor

The system shown in Figure 1 is a unique concept as it eliminates (i) conduction heat loss along TE elements with unused heat carried back into the combustion process by gas stream convection, (ii) thermal contact resistances, which are a major impediment in conventional TE power generation designs.

This approach presents a series of innovations enabling portable power generation systems. The system is not severely affected by conductive heat losses within TE materials as in conventional TE power generation modules. Optimization of the TE materials will focus on the power factor, $PF = S^2\sigma$, with materials optimization avoiding the decades old challenge of minimizing thermal conductivity and maximizing electrical conductivity.

CHAPTER 2: BACKGROUND INFORMATION

2.1 Introduction to Combustion

Combustion processes are a complex series of chemical reactions between a fuel and an oxidant that produce heat at enormous energy densities per unit weight of fuel consumed (40-60 MJ/kg):

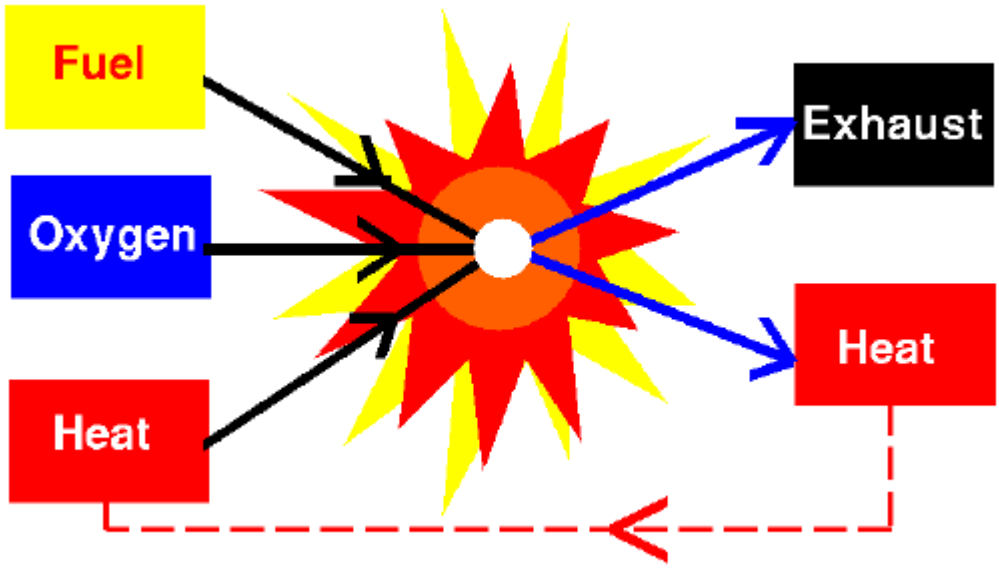

Figure 2: Illustration of Combustion (Scott)

The chemical formula of the reaction used is as follows:

$CH_4 + 2O_2 \rightarrow CO_2 + 2H_2O + Heat$

A ceramic material was chosen to make a microcombustor for this project because it has good mechanical stability as well as high thermal and chemical resistance to withstand the high temperature reactions taking place (~1000°C). The procedure for the manufacturing of this ceramic device, as well as more information about the material itself is described in Chapter 4 (Kenis).

2.2 Introduction to Thermoelectrics

Thermoelectricity is the direct conversion of heat to electricity. A temperature gradient is applied to a p-type/n-type configuration to generate a voltage, and a heat flux is applied to maintain this temperature gradient, illustrated below:

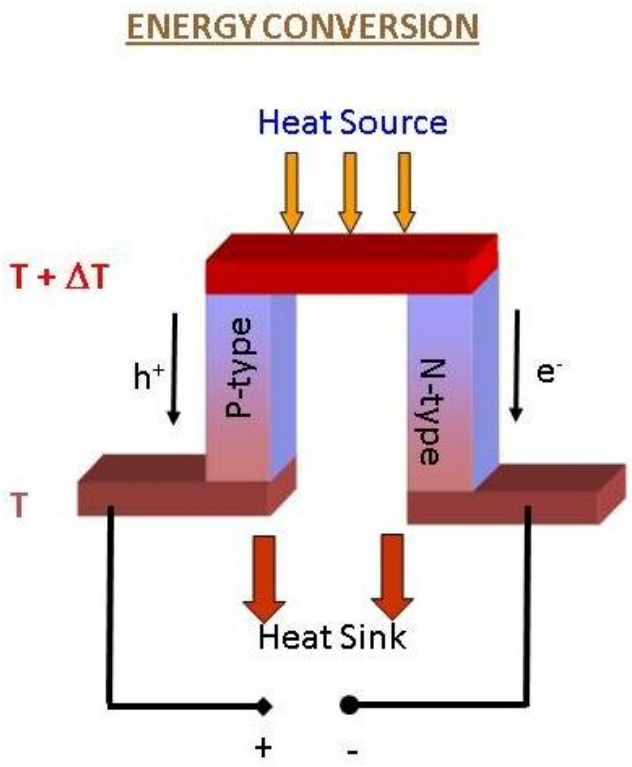

Figure 3: Thermoelectric Schematic ("Environmental Engineering at UCSD")

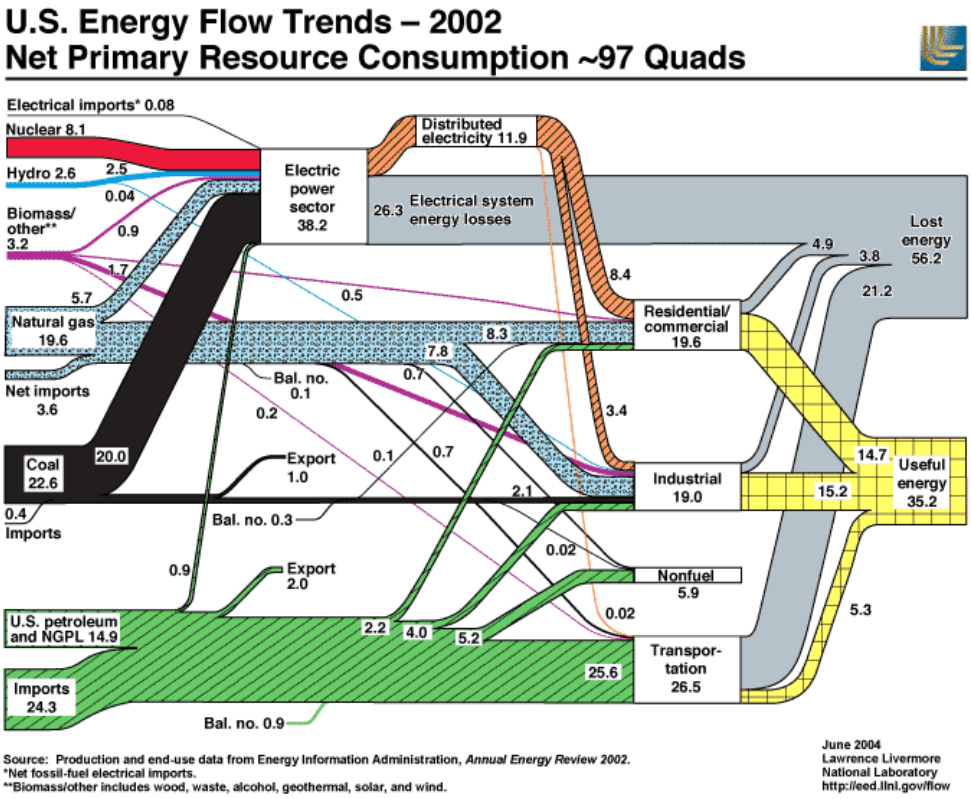

Figure 4: U.S. Energy Flow Trends in 2002

See Figure 4 above for U.S. energy flow trends in 2002 ("U.S. Energy Flow – 2002"). The left side of the chart shows sources of energy. The combustor device falls into the "Natural Gas" category since it requires methane. More significantly, the right side of the chart shows that 56.2% of used energy is lost. What thermoelectric devices do is turn the wasted heat from the combustor into useful energy (on the chart, 35.2%).

There are many benefits to a thermoelectric device. First of all, a thermoelectric device requires very little maintenance because there are no moving, mechanical parts. This means that they have a virtually unlimited lifespan. The devices are also very scalable (1W-1kW), meaning they can be used for a range of purposes. Thermoelectrics also allows for a high energy density per weight of fuel consumed: 2-10% conversion of hydrocarbon fuels offers more energy density

than a lithium battery, even taking into account different energy types and converting thermal to electrical energy. Also, lithium batteries are causing environmental problems since they are unable to be easily recycled. Moreover, waste heat can be used to run these thermoelectric configurations, such as how cars are beginning to use exhaust heat to make electricity. Also, TE devices are being used in cars for seat cooling in the summer (using battery electricity). Other uses of applying thermoelectrics to waste heat include power plants and pocket stoves (Yoshida). Lastly, a thermoelectric device can be inverted by running a current across and allowing it to act as a heat pump instead. These devices are important because they have the potential to reduce carbon dioxide and other greenhouse gas emissions by reducing fossil fuel use (Bell).

Yoshida describes how to achieve maximum output power of thermoelectric generation using the following equations:

$$P_{\max} = \frac{\alpha^2 \Delta T^2}{4R} = \frac{1}{4R}\frac{\alpha^2}{\rho\kappa}\frac{\kappa A}{L}\frac{\rho L}{A}\Delta T^2 = \frac{ZK\Delta T^2}{4}$$

$$Z = \frac{\alpha^2}{\rho\kappa}, \quad K = \kappa\frac{A}{L} \text{ and } \quad R = \rho\frac{L}{A}$$

In the above equations, Z is the figure of merit, K is the total thermal conductance, and ΔT is the temperature difference between the hot and cold junction. Also, R is the internal resistance of the TE module, κ is the thermal conductivity, A is the cross sectional area of the TE elements, L is the length of the TE elements, α is the Seebeck coefficient of the thermocouple, and ρ is the resistivity. As the temperature difference increases, power output (P_{max}) increases which is why

combustion was chosen to be used in conjunction with thermoelectric generation: combustion greatly increases the temperature difference to maximize this power output, especially since this temperature difference is squared. (See information/discussion above)

A more commonly seen equation used to determine the efficiency of a thermoelectric generator is as follows:

$$zT = T\frac{S^2\sigma}{\kappa}$$

In the above equation, S is the thermoelectric power (Seebeck coefficient), T is the absolute temperature, σ is the electrical conductivity, and κ is the thermal conductivity. The zT quantity is called the figure of merit: the higher the zT value, the more efficient the thermoelectric generator. This is the single most important parameter that determines the efficiency of a TE device (Heremans).

Despite the advantages to thermoelectricity discussed above, many scientists believe its uses will be limited to applications that do not run efficiently on existing energy sources or do not run at all presently. This is because the efficiency of thermoelectric generators at high power levels is much less than steam generators today:

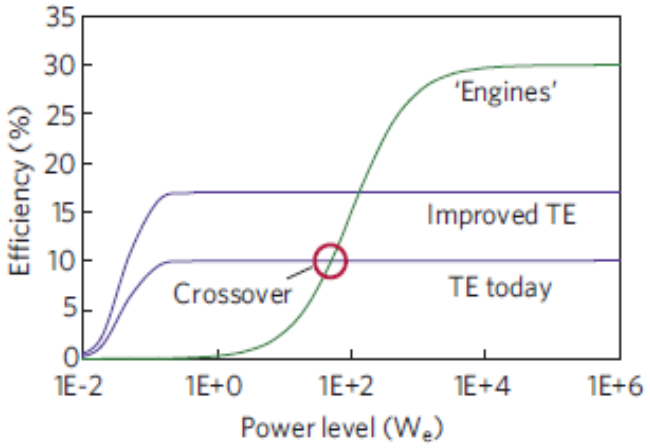

Figure 5: Comparison of TE devices and Steam Engines (Vining)

TE devices with *ZT* = 0.7 are commercially available today (though it is believed material optimization will allow a *ZT* of 3 in the near future). However, low efficiencies do not mean we should stop researching TE technology: it is still useful in applications that improve fuel efficiency such as car air-conditioning and the waste heat recovery mentioned earlier. The reason for that is that the more efficient steam cycles also require larger and heavier machines, and the energy recovered does not pay for the energy needed to carry them aboard the vehicle. Figure 5 shows how the overall efficiency of different technologies scales with the power level of the machines: thermoelectric converters are better at lower power levels. Honda has increased engine efficiency by 3.8% with waste heat recovery, and BMW has improved fuel efficiency by 5.5% by adding thermoelectric waste heat recovery to their power train. So though thermoelectricity may not solve the energy crisis for large scale applications such as replacing an entire steam engine, it can greatly increase fuel efficiency by using the devices in conjunction with existing technologies. TE technology is best adapted to energy conversion in small systems (Vining).

The p-type and n-type material that are connecting electrically (see Figure 2) are together called the thermocouple. These are two metals or semiconductors made by a doping process, in which a material takes on a negative charge (n-type) or positive charge (p-type). Impurities are added to the materials to create either free electrons or an absence of electrons which are called "holes" (Brain). "It is well known that TE films with high Seebeck coefficients (and opposite in sign), low thermal conductivity, and low electrical resistivity are desired for high TE conversion efficiency" (Boniche). However tradeoffs must be made due to physical constraints, electrical contact reliability, and material availability. The optimizations applied to this project will be discussed in Chapter 5, the Results section.

The radial design that is being used for this integrated combustor/thermoelectric device allows for the hottest temperature to be in the center and coolest on the outer edges (see Figure 4 below). Three channels are being used so that there is no premixing of the gases. This is to control the location where the combustion starts, and move it to the center of the combustor. Also, if the combustion reaction is too hot (could heat up to 2200°C), the ceramic will melt. The heat conducted by the integrated thermocouple will be brought back into the combustion process by convection. This radial design maximizes both the Seebeck voltage $\Delta V=\alpha\ \Delta T$ and the Carnot efficiency: $\eta = 1 - \frac{T_{cold}}{T_{hot}}$ ("Carnot Cycle", "Temperature Prelab Lecture"). The heat from the combustion is expected to increase the efficiency by increasing T_{hot} (for the same cold junction temperature). Moreover, the greater the temperature difference between T_{hot} and T_{cold}, the greater the voltage output according to the Seebeck effect, and the overall power of the device will scale with $(T_{hot}-T_{cold})^2$. The Seebeck coefficient (α) is a material property based on the

chemical nature of the thermocouple and also the temperature range spanned by the thermocouple during operation.

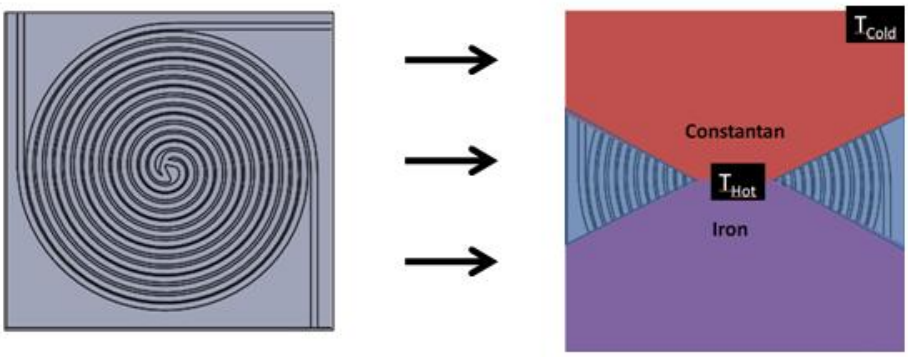

Figure 6: Radial Gradient design

The Carnot efficiency equation above $\eta = 1 - \frac{T_{cold}}{T_{hot}}$ comes from the Carnot cycle, the most effective heat engine cycle (Nave). The Carnot Cycle is made up of two isothermal processes and two adiabatic processes, and is illustrated by the following:

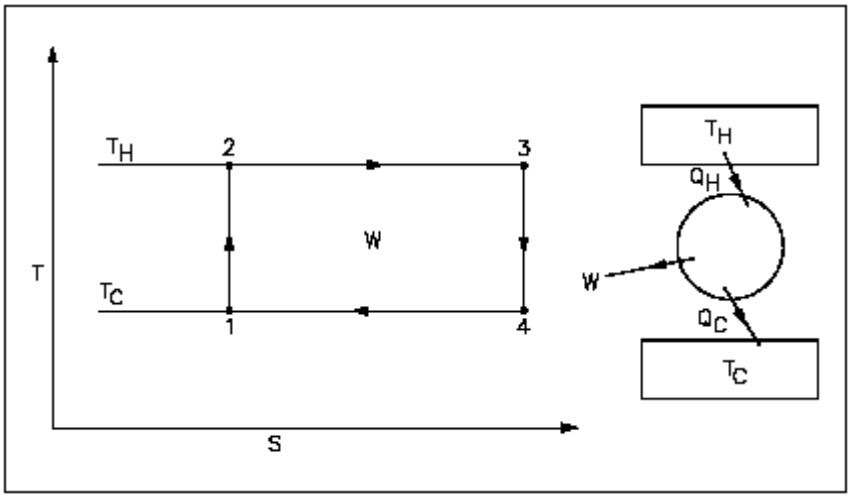

Figure 7: Carnot Cycle Representation ("Carnot Cycle")

In the figure above, *T* represents Temperature and *S* represents entropy, the measure of disorder in a system.

CHAPTER 3: PAST WORK

Kenis's article gives suggestions and descriptions for fabrication ceramic microstructures, such as the one used in this thesis project to make the microcombustor. It is stated in this article that "Ceramics are attractive materials for engineering applications involving high temperatures and corrosive chemicals", such as combustion. Moreover, it is "inexpensive and reproducible" which is useful when designing and iterating on the design to improve it. Kenis uses a similar gelcasting procedure that this paper describes in chapter 4 to form a ceramic device. Gelcasting is used rather than the usual slip casting or dry pressing to make ceramics because gelcasting allows the green bodies to have higher density, higher strength, and greater homogeneity (Kenis). The main idea taken from this paper was the use of a dispersant (Darvan 821A, R.T. Vanderbilt, Norwalk, CT). This addition is further described in the Results Chapter. Kenis also describes how the alumina slurry was dried in a PDMS mold, in a similar procedure described in the Experimental Procedures Chapter.

Yoshida's article discusses the reasons one would combine combustion with a thermoelectric generator. The article describes how the efficiency of a catalytic butane combustor was tested both with and without a thermoelectric generator. A similar setup is used for this project, except that in Yoshida's work the thermoelectric generator is completely separated from the fuel, air and products, the fuel and air are premixed, a catalyst is used, and an ignition heater is used to start combustion rather than a match. Our system integrates TE and combustion.

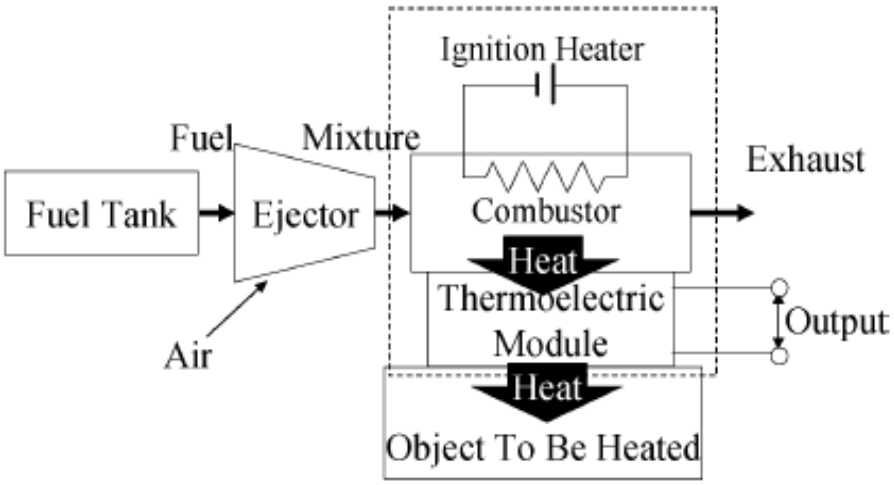

Figure 8: Diagram of sample TE generator/combustor unit

Similarly to the process followed in this thesis, Yoshida's experiment was first performed without the TE generator, and then the module was added once the combustion was properly stabilized. Unlike Yoshida's experiment, it was decided that the gasses should not be premixed for this thesis project because the mixing point determines where the combustion occurs. In our case, the combustion is meant to occur at the center, so this is where we mix air and fuel. Moreover, if the reaction was too hot (much greater than the expected 1000 degrees Celsius), the thermocouple would melt. Yoshida also uses a BiTe system which is a common and efficient thermocouple, though not readily available in the foil form that was needed for this project, not suitable for operations above 200 ^{o}C, and not sufficiently chemically resistant to be exposed to air at high temperature. The catalysts were used in this setup to allow for stable combustion in a small space at relatively low temperatures; they are not necessary for this thesis, because the combustion temperature is higher. The setup described in Yoshida's article achieves an efficiency of 2.8%. Another aspect of this article useful for this thesis was the energy losses to

account for and minimize if possible. These include unreacted fuel, heat loss through conduction of unconverted heat down the thermocouples, convection in the product gases, and radiation (Yoshida).

CHAPTER 4: EXPERIMENTAL PROCEDURES

4.1 Molds

The general procedure for making the microcombustor was to first make a copy of the device out of brass, use a PDMS countermold that is a negative of the device, and then pour the ceramic into the PDMS to achieve the final piece:

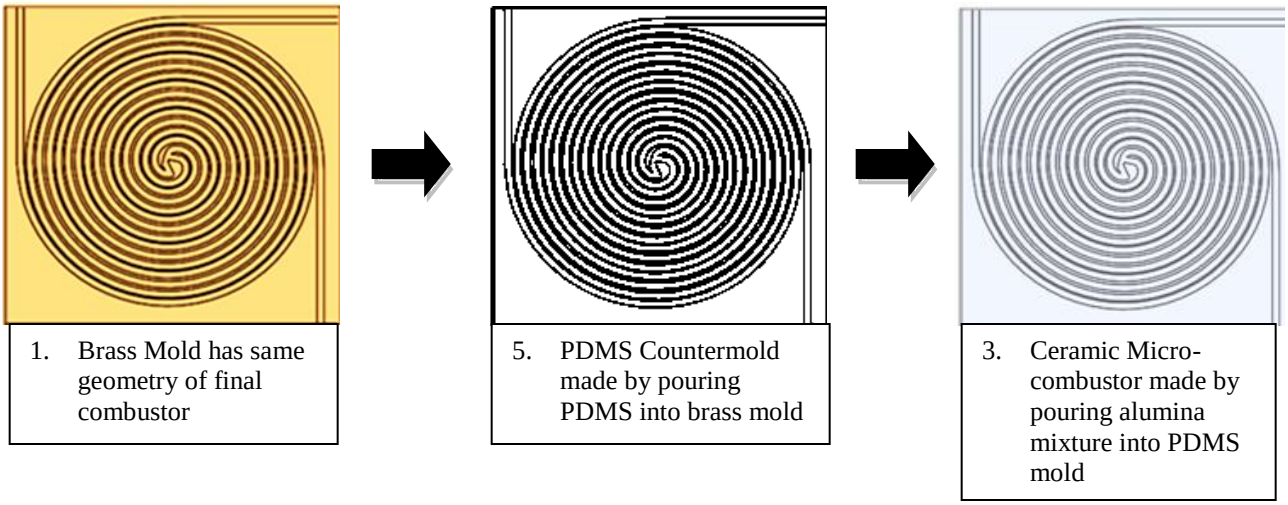

Figure 9: General Procedure for Combustor Fabrication

The reason for so many steps is because the ceramic material (sintered alumina) needed to withstand combustion is too brittle to be directly machined. Also, machinable alumina (macor) is porous and prone to gas leaks in addition to being brittle.

4.1.1 Brass Mold

This piece was machined out of brass. There were three iterations of this piece made due to changes in geometry (to be discussed in 5.1, Recipe Development of the Results chapter). The first two molds were machined at the ISE machine shop in Baker Systems, and the last at the Scott Lab Machine Shop.

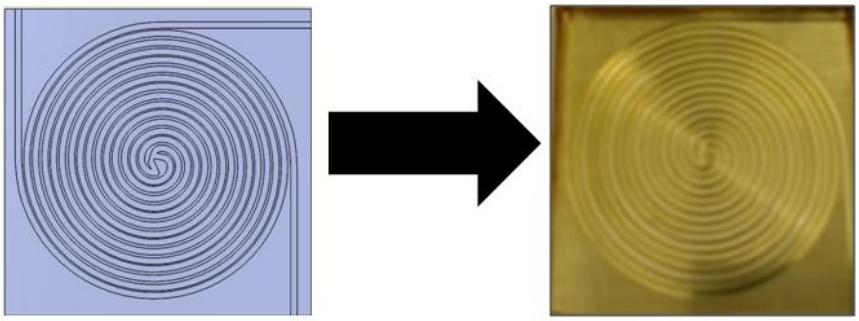

Figure 10: Brass Mold Design

4.1.2 Silicon Elastomer Countermold

A Silicon Elastomer called Polydimethylsiloxane (PDMS) was utilized to make the countermold of the ceramic combustor. First, the elastomer and curing agent were mixed in a 10:1 ratio (Sylgard© 184 Silicone Elastomer Curing Agent and Base, DOW CORNING). Then, a vacuum was used to remove air bubbles (optimum cycle time to remove all air bubbles: 8 cycles at 7 minutes each). Then, the mixture was poured into the brass mold shown in the figure above, with copper tape lining the edges of the mold to contain the mixture. The entire piece was then set on a burner to cure. The total process time was 3 hours per sample, though this countermold was able to be reused if the ceramic device was fully removed (see 4.2.1). See Appendix A for the process sheet used for this procedure.

4.2 Combustion

4.2.1 Ceramic Microcombustor

A gel-casting procedure was used to produce a high density sintered alumina device (0.95 g/cm^3) that can withstand 1000°C or higher combustion temperatures (For photos, see Chapter 5). This was made by first mixing polyvinyl alcohol (99% hydrolyzed, Aldrich Chemistry), water, and high purity alumina powder (CR 1, Baikalox) with a magnetic stirrer while on the burner. The mixture was then poured into the PDMS countermold and air bubbles were removed with the vacuum. The whole piece was then air-dried and then dried on the burner. The ceramic piece could then be separated from the PDMS and placed in the furnace. The furnace process used is represented below (~50 hours total):

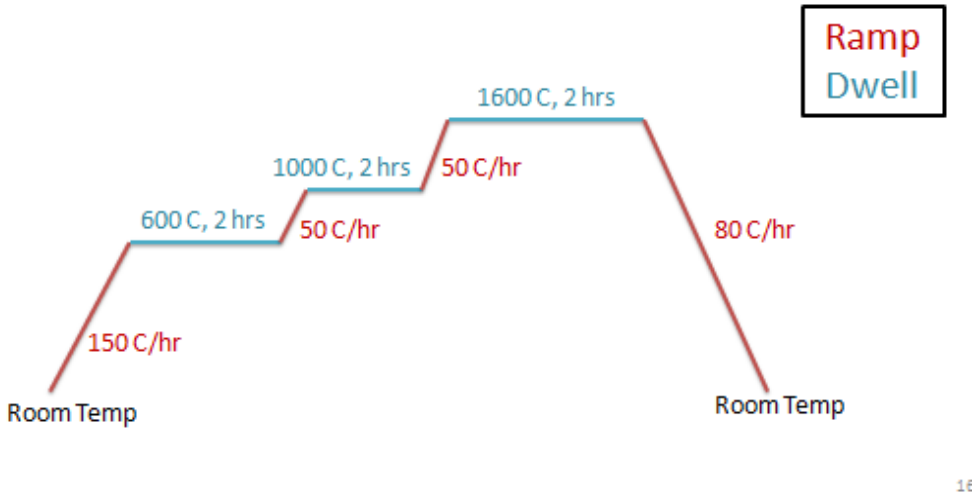

Figure 11: A process flow diagram for the furnace process that sinters the alumina device.

The total process time for fabricating a test combustor is 8-12 days, depending on air drying time. For a more detailed procedure used for this process, see Appendix A. This gel-casting procedure was able to provide good mechanical stability which allowed this micro-scale device to withstand high temperatures (crystal particle size of 1.1 µm, ultimate particle size 600 nm, pore volume 1 ml/g).

The following schematic shows the design of the microcombustor and its different parts:

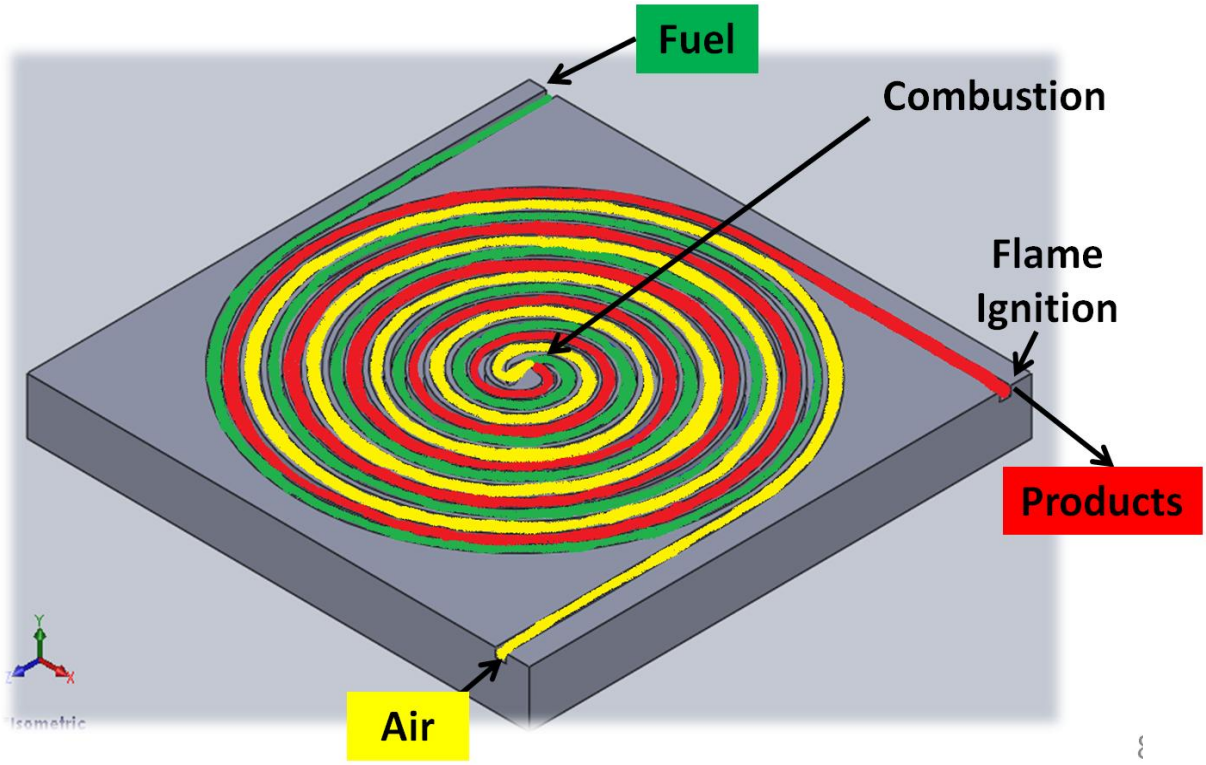

Figure 12: Combustor Design

This was designed to have three channels that are compacted into a 2.25”x2.25” design to result in a radial temperature gradient, as described in Chapter 1. The fuel and air are the two input channels shown in green and yellow above, and the products (as well as the flame ignition) are in the output channel shown in red. The center of the spiral, where all three channels meet, is shown zoomed in the figure below:

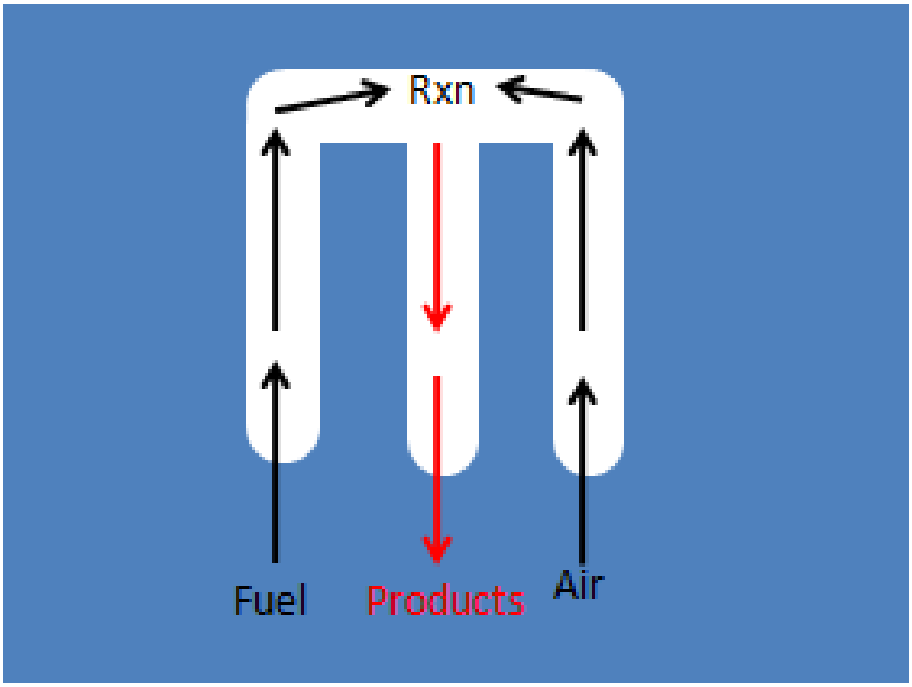

Figure 13: Combustion occurs in center where three channels (spirals) meet

4.2.2 Combustion Gases

The fuel used for combustion was 99.0% methane, and the oxidant was 99.0% compressed oxygen.

4.3 Thermoelectrics

The thermocouple chosen to test the heat-electricity conversion efficiency was Iron-Constantan due to its availability in foil form, its excellent mechanical properties, its reasonably good corrosion resistance at high temperature, and its high thermopower *S* for the two metals. The p-type was the Iron (0.001" thickness, purity 99.5%, Alfa Aesar) and the n-type was Constantan (0.001" thickness, Reade Advanced Materials). Constantan is a Copper-Nickel alloy composed of 53.8% Copper, 44.2% Nickel, 1.5% Manganese, 0.5% Iron

("Constantan Foil/Sheet/Wire from READE"). The foil was laser welded along a line in the middle as shown below:

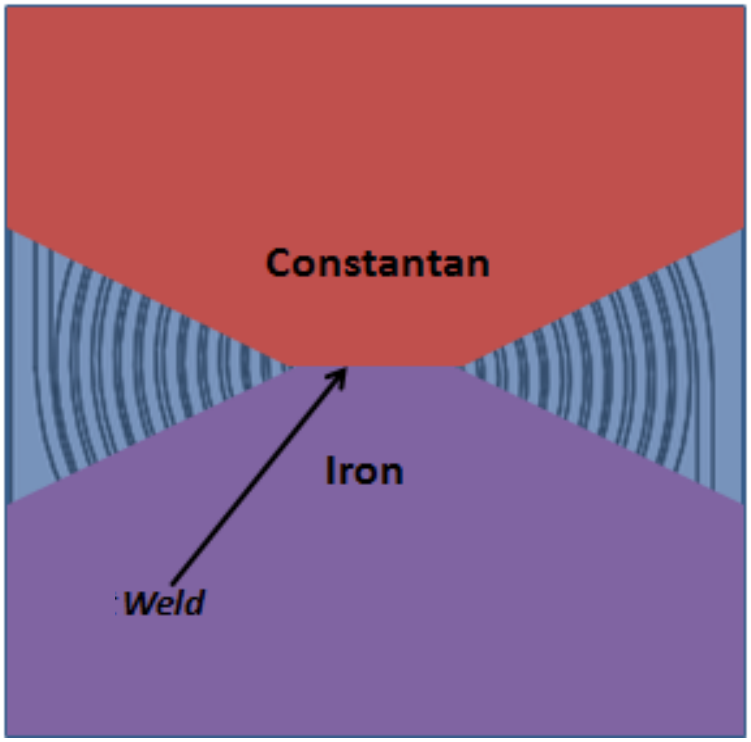

Figure 14: Integrated Thermocouple

The combustor was sealed by a 1/16" thick quartz sheet the same length and width of the combustor itself, fastened with ceramic glue (Ceramabond 671, Aremco). Spaces were left for the channel exits to attach tubing for the gases. The outside edges of the constant and iron were then attached to the top of the quartz with the ceramic glue. High-alumina ceramic tubing (0.125" OD, 0.063"ID, 1" long each, McMaster-Carr) was used for the two channels used to input the oxygen and methane. FEP tubing attached between the ceramic tubing to mass flow controllers (MKS Type 1179A General Purpose Mass-Flo Controllers). The input ends of the mass flow controllers were attached to ½" stainless steel tubing, which ran the gases from the tanks. A mass flow digital readout was connected to the mass flow-controllers, and a voltmeter

was used to read the output voltage by attaching alligator clips to the thermocouple. See Chapter 5 for photos of each variation of the setup described.

CHAPTER 5: RESULTS

5.1 Recipe Development – Combustor Fabrication:

A successful recipe was developed for a ceramic gel-casting process by adjusting different steps to build an alumina green body (See Appendix A for detailed procedure). First, the polyvinyl alcohol-to-water ratio was decreased so that the alumina slurry was well-mixed with an appropriate viscosity. The original ratio used was 2 grams PVA for every 10 mL water, and in the end became 1.6 grams PVA for every 15mL water to end up with a less viscous solution.

However, once the alumina powder was added, the mixture was still very thick, clumpy, and hard to pour into the PDMS mold. Darvan 821A (R.T. Vanderbilt, Norwalk, CT) is a commercial dispersant that was added to allow for the alumina to mix more thoroughly, without particle aggregation or "clumping" (Kenis). The paper suggests adding Darvan in the amount of 2 wt% of the total alumina powder used, though this caused the solution to have a watery consistency. Thus1 wt% was tried and found to be most successful at eliminating clumps.

The geometry of the combustor was also modified several times. The channel size was increased over the 3 versions (see Appendix B), and the number of turns each channel made was decreased in Geometry 2 to decrease the wall breakage that was occurring with the ceramic material. Also, Geometry 2 was made using the 3D prototype printing machine, though the resolution was too grainy compared to the brass mold, and resulted in a PDMS mold with many surface defects.

An additional problem that needed to be solved is the warping of the ceramic green body as it goes through the drying process. This has been reduced by allowing the body to cure on a metal plate.

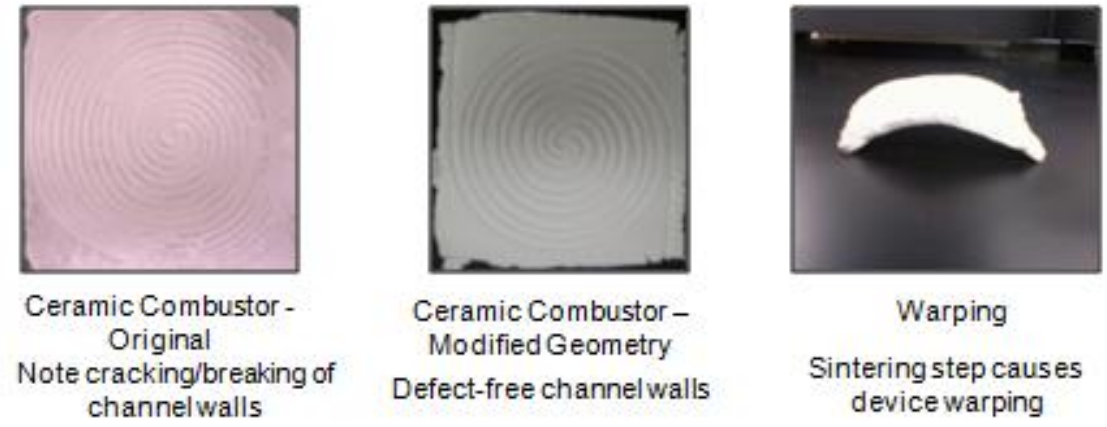

Figure 15: Ceramic Gel-Casting Selected Results

5.2 Thermoelectric Integration

5.2.1 Combustion Process Set-up #1 - Y-combustor

As a model system to test the operation of the testing station, we used a Y-shaped combustor with three laser-machined microchannels:

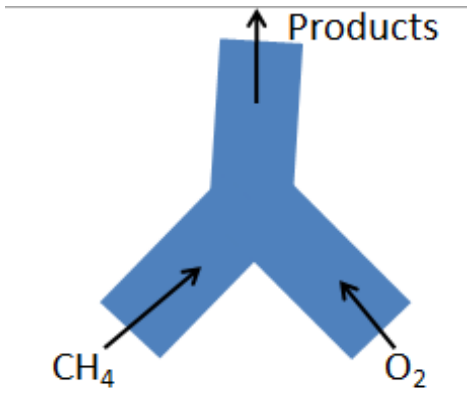

Figure 16: Y-Combustor with 2 input channels (methane and oxygen) and 1 output channel

In this set-up, the mass-flow controllers were utilized with the methane and oxygen flows so that a stabilized flame was produced using a simple Y-shaped microcombustor. The thermocouple was integrated to obtain a voltage:

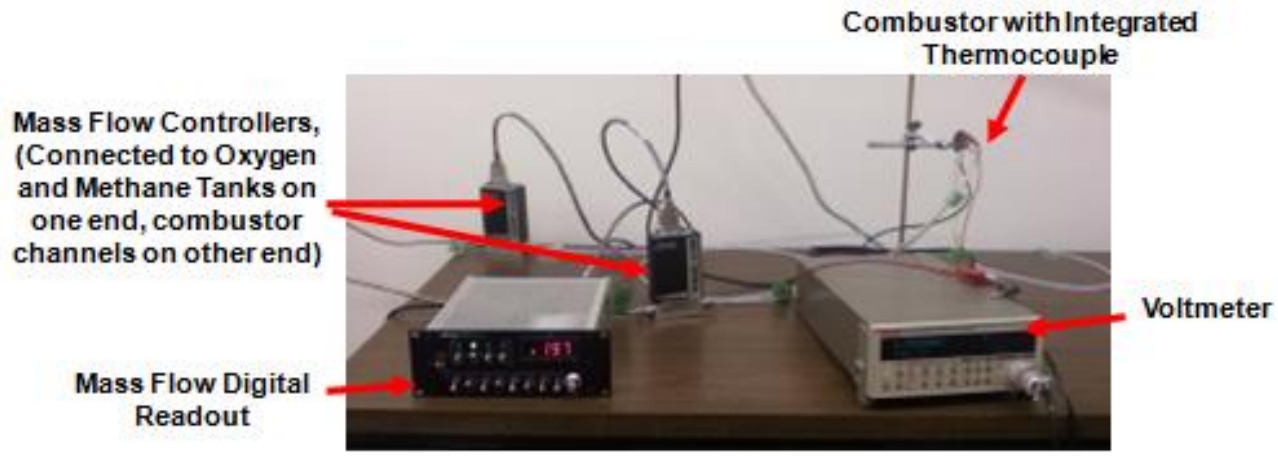

Figure 17: Combustion and Thermoelectric Integration Setup #1 – Y-Combustor

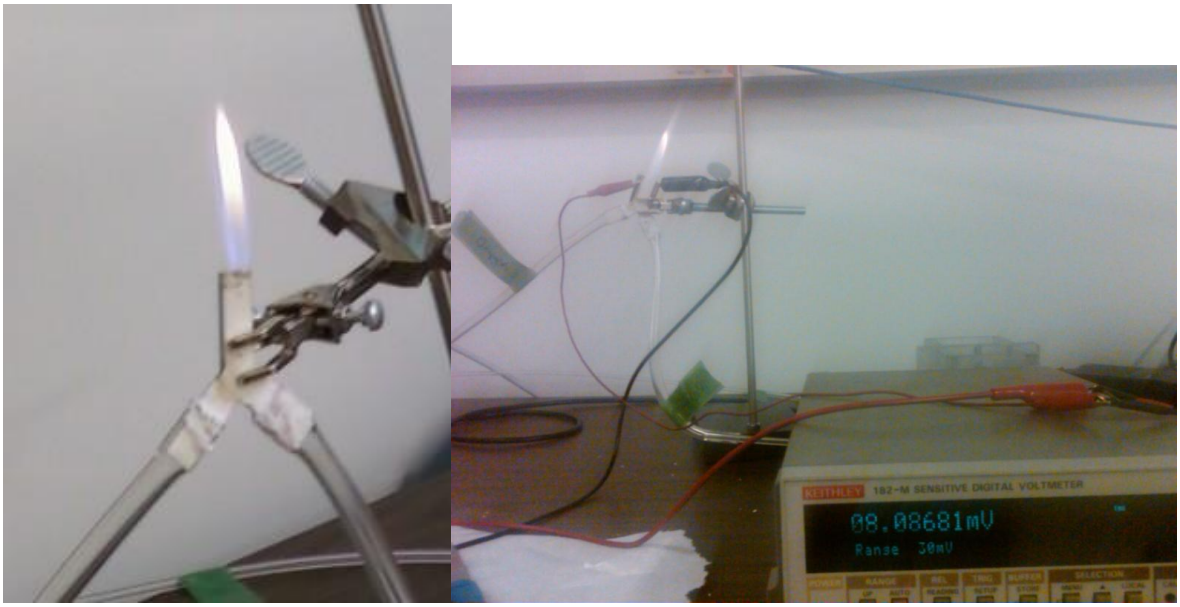

Figure 18: Y-Burner Photographs

Table 1 is the first set of data obtained using the Y-Burner. From 0 to 7.25 seconds, an outside flame was visible. At 7.25 seconds, the external flame was extinguished but the internal flame inside the combustor was still burning.

Table 1: Y-Combustor Data – Methane at 200 sccm, Oxygen at 200 sccm (June 4, 2010)

Time (min)	Voltage (mV)
0	Outside flame, 0.008
0.5	--
1	7.90
1.5	8.60
2	9.12
2.5	9.64
3	--
3.25	9.83
4	10.20
4.5	10.34
5	10.46
5.5	10.34
6	10.18
6.5	10.17
7	10.03
7.25	Extinguished, 10.09
8	10.25
8.5	10.40
9	10.28
9.5	10.30
15	10.69

As shown, the maximum voltage obtained was 10.69 mV at 15 seconds. It was determined that since the goal was to obtain 75 mV, the next step to increasing efficiency is to weld the thermocouple together (rather than just gluing them as they were above). The weld would decrease contact resistance by decreasing overlap significantly.

A disc-laser weld was performed at the Edison Welding Institute in Columbus, Ohio. The weld used caused the spot to mix into an Iron-Constantan alloy with unknown concentrations. However, since this alloy has a constant temperature (T_{HOT} in Figure 6), this does not add or take away from the electric potential:

$$\mathbf{V} = \mathbf{S}_{CONSTANTAN} \times (\mathbf{T}_{COLD}\text{-}\mathbf{T}_{HOT}) + \mathbf{S}_{UNKNOWN} \times (\mathbf{T}_{HOT}\text{-}\mathbf{T}_{HOT}) + \mathbf{S}_{IRON} \times (\mathbf{T}_{HOT}\text{-}\mathbf{T}_{COLD})$$

$$\mathbf{V} = (\mathbf{T}_{HOT}\text{-}\mathbf{T}_{COLD}) \times (\mathbf{S}_{CONSTANTAN}\text{-}\mathbf{S}_{IRON})$$

where S is the Seebeck coefficient for the given materials.

5.2.2 Combustion Process Set-Up #2 – Spiral Combustor (Without Thermocouple)

Next, a similar configuration to set-up #1 was used, as shown in the Figure below:

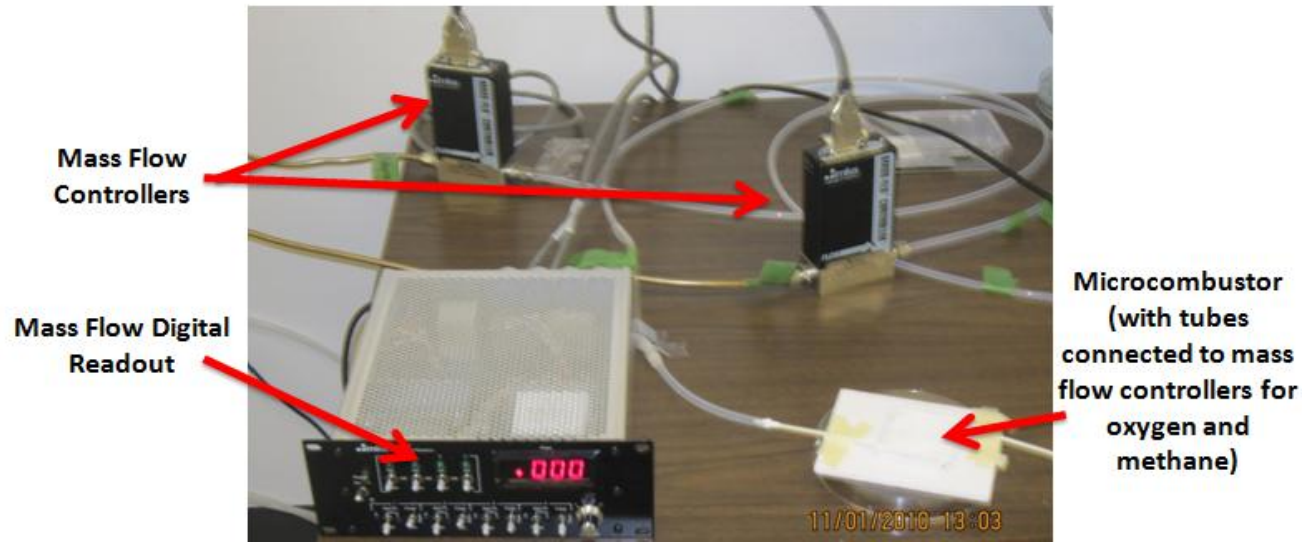

Figure 19: Combustion Process Setup #2 - Spiral Combustor

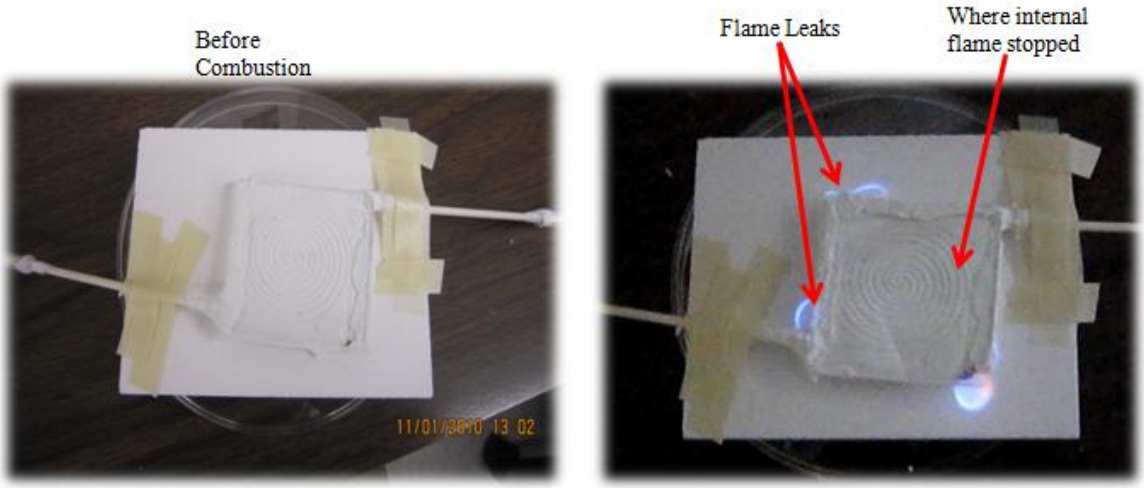

Figure 20: Spiral Combustor Before and after testing (Set-up #2 - Without Thermocouple)

Leaking of the gases occurred repeatedly, most likely underneath the combustor. This caused the flame leaks shown in the figure above. Moreover, the walls between the channels were not able to be fully sealed due to warping of the ceramic; the quartz was not flush with the combustor piece, so that the fuel and oxidant mixed at various locations in the combustor instead of only in the middle and temperature gradient was not radial, as by design. Due to these reasons along with a reaction temperature of less than 200°C, the flame only traveled approximately two inches back into the products channel before stopping. The next step was to add the thermocouple device and observe the voltage obtained.

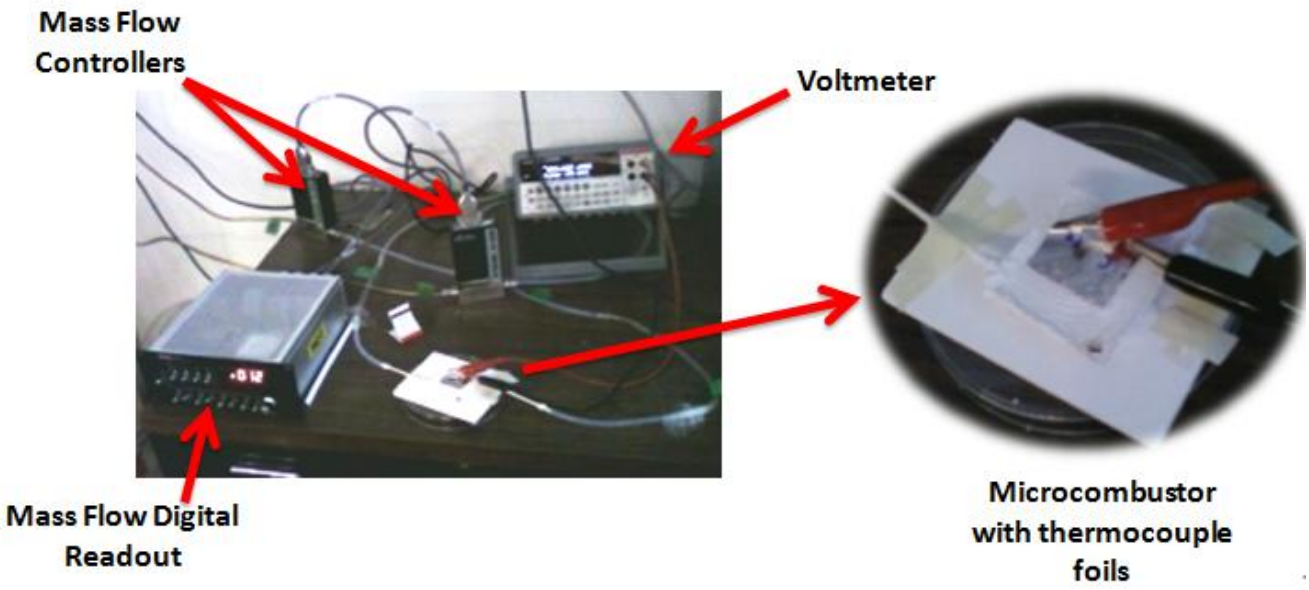

Figure 21: Combustion Process and Integrated Thermocouple Set-Up #3 - Spiral Combustor

The thermocouple foils were added as shown above, with the laser weld along the seam of the two foils in the center of the device. The foil did not reach the edges of the combustor as the original design intended since leaks occurred along these areas.

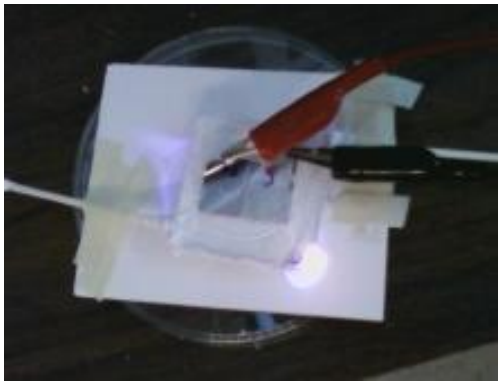

Figure 22: Combustor with integrated thermocouple during testing

The following voltages were obtained for Set-up #3:

Table 2: Spiral Combustor Data --Methane at 200 sccm, Oxygen at 200 sccm (November 5, 2010)

Time (min)	Voltage (mV)
0	Outside flame, 0.045
0.5	0.068
1	0.10
1.5	0.22
2	0.36
2.5	0.51
3	No flame, 0.67
4	1.06

It was concluded that when the "hot spot" of the combustion is not in the center of the design as explained previously with the desired temperature gradient, a maximum voltage cannot be obtained. The warping of the ceramic combustor needs to be decreased and the channels sealed more fully.

CHAPTER 6: FUTURE WORK AND CONCLUSIONS

The overall future goal for this line of research is to create a combustor/thermoelectric group the same voltage of a C-cell battery that could be used in potential applications such as a portable power supply for the army. Suggestions for next steps in this project are to continue to decrease warping of the ceramic device so that the channels can be sealed completely. Also, a next step could be to perform a study of the temperature profile using either thermocouples with temperature readout and/or an infrared camera. Moreover, the portability of the design could be studied and improved. Then 20 of these devices could be stacked into a pile, and connected thermally in parallel and electrically in series to form a 1.5V power supply about the size of a C-cell but with a much higher energy capacity. It would also require to a cartridge design for the methane and oxygen, along with a system to contain the flame/heat to make the complete assembly portable and safe.

In conclusion, an integrated system with direct heat to electricity conversion was demonstrated. As expected this portable power system provided a high density power source by conversion of the high energy density of conventional fuel source for portable energy needs.

WORKS CITED

Bell, L. E. "Cooling, Heating, Generating Power, and Recovering Waste Heat with Thermoelectric Systems." *Science* 321.5895 (2008): 1457-461.

Boniche, Israel, Sivaraman Masilamani, Ryan J. Durscher, Brian C. Morgan, and David P. Arnold. "Design of a Miniaturized Thermoelectric Generator Using Micromachined Silicon Substrates." *Journal of Electronic Materials* 38.7 (2009): 1293-302.

Brain, Marshall. "How Semiconductors Work" 25 April 2001. HowStuffWorks.com. <http://electronics.howstuffworks.com/diode.htm> 03 October 2010.

"Carnot Cycle." *Engineers Edge - Design, Engineering & Manufacturing Solutions*. Engineers Edge, LLC. Web. 29 Dec. 2009. <http://www.engineersedge.com/thermodynamics/carnot_cycle.htm>.

"Constantan Foil/Sheet/Wire from READE." *READE Advanced Materials*. Web. 18 Oct. 2010. <http://www.reade.com/Products/Alloys/constantan_foil_sheet.html>.

"Environmental Engineering at UCSD." *UCDS Jacobs: Mechanical and Aerospace Engineering*. University of California, 2009. Web. 29 Sept. 2009. <http://maeweb.ucsd.edu/enviroeng>.

Heremans, J. P., V. Jovovic, E. S. Toberer, A. Saramat, K. Kurosaki, A. Charoenphakdee, S. Yamanaka, and G. J. Snyder. "Enhancement of Thermoelectric Efficiency in PbTe by Distortion of the Electronic Density of States." *Science* 321.5888 (2008): 554-57.

Kenis, Christian, and Paul J.A. Kenis. "Fabrication of Ceramic Microscale Structures." *Journal of the American Ceramic Society* 90.9 (2007): 2779-783. *Wiley Online Library*. John Wiley & Sons, Inc, 7 July 2007. Web. 1 Oct. 2009. <http://onlinelibrary.wiley.com/doi/10.1111/j.1551-2916.2007.01840.x/pdf>.

Nave, R. "Carnot Cycle." *HyperPhysics*. Web. 03 Oct. 2010. <http://hyperphysics.phy-astr.gsu.edu/hbase/thermo/carnot.html>.

"Temperature PreLab Lecture." Me 570 Lab. Scott Lab at OSU, Columbus. Winter 2010. Lecture.

Scott, Jeff. "Ask Us - Jets and Rockets." *Aerospaceweb.org: Reference for Aviation, Space, Design, and Engineering*. 1 Feb. 2004. Web. 29 Sept. 2009. <http://www.aerospaceweb.org/question/propulsion/q0161.shtml>.

"U.S. Energy Flow – 2002" Energy and Environment at Lawrence Livermore National Laboratory. 28 February 2005. 12 February 2009 <https://eed.llnl.gov/flow/02flow.php>.

Vining, Cronin B. "An Inconvenient Truth about Thermoelectrics." *Nature Materials* 8.2 (2009): 83-85. Print.

Yoshida, K., S. Tanaka, S. Tomonari, D. Satoh, and M. Esashi. "High-Energy Density Miniature Thermoelectric Generator Using Catalytic Combustion." *Journal of Microelectromechanical Systems* 15.1 (2006): 195-203.

Prakash, Shaurya. Procedure for "Ceramic Gel Casting – Version 3." Ohio State University. February 2010.

Prakash, Shaurya. Procedure for "PDMS Molding – Version 1." Ohio State University. February 2010.

APPENDIX A - PROCEDURES

Procedure for PDMS Molding

1. Measure 20 g silicon elastomer into a plastic cup.
2. Add 2 g curing agent (1:10 ratio by weight).
3. Stir mixture in 1 direction for 10 minutes with spoon.
4. Set burner to 75°C about ten minutes before use.
5. Place mixture in the plastic cup inside the vacuum desicator. Vacuum for 5-7 minutes, then atmospheric release. Repeat cycle until there are no more air bubbles.
6. Slowly pour mixture into desired mold. Remove air bubbles created if necessary.
7. Allow mixture to cure on the burner for 2 hours (75°C).

(Prakash)

Original Procedure for Gel Casting Alumina

1. Prepare aqueous PVA solution by dissolving 2 g of PVA in 10 mL of DI water for 3 hours under constant magnetic stirring at 85-90^{0}C (Note: Observe that a clear liquid solution is obtained).
2. Add 8 g of Alumina powder into the PVA solution to obtain suspension. The mixture is magnetically stirred at 85^{0}C for at least 24 hours (Note: The idea of longer stirring is to de-agglomerate the alumina powder, disperse the powder into the solution and obtain a better mixture).
3. Add 2 g of Maleic acid to cross-link the alumina suspension. Mix thoroughly and stir for half an hour at 85^{0}C.

4. Pour the alumina suspension into the PDMS mold and degas under the vacuum annealer.
5. After degassing, heat cure the lamina suspension under vacuum at 160^0C for 5 hours.

Degassing (under iterations):

6. Turn on the hot plate and set the temperature at 85^0C. Turn on the vacuum pump and turn off the pump when the gauge meter reads -28 in Hg.
7. Release N_2 gas into the vacuum chamber after 5 minutes to obtain a gauge reading of -20 in Hg. Stop N_2 gas release. Next, turn on the pump until the gauge reaches -28 in Hg. Turn off the pump and repeat release N_2 gas process for the next 3 times.
8. Repeat step 2 by varying the time step to 15 minutes instead of 5 minutes for the next 3 times (Note: Increase the vacuum by increasing the gauge reading to -29 in Hg or -30 in Hg to remove the air bubbles).

(Prakash)

Final Procedure for Gel Casting Alumina

1. Measure 1.6 g Polyvinyl Alcohol (PVA) and transfer to scintillation vial
2. Add 15 mL water to the vial
3. Put a magnetic stirrer in bottle and screw on the lid. Place on hot plate at 85°C for 2 hours, set stir to 700 rpm. If all of the PVA is not fully dissolved after 2 hours continue stirring till all PVA is dissolved
4. Measure 2.3 g Al_2O_3 powder (*Note*: We have two different particle sizes, use the one for your device)
5. Remove vial from hot plate and add Al_2O_3 powder from Step 4.
6. Screw lid back on, and place back on hot plate at 85°C stirring at 700 RPM for 10 min.

7. Repeat Steps 4-6 three more times until total 9.2 g of Al_2O_3 powder have been added
8. Let the bottle sit on the hot plate at 85°C stirring at 700 RPM for 24 hours
9. Measure 1.6 grams Maleic acid under fume hood and add to vial (*Note*: Maleic acid is a cross-linking agent for PVA and with the warm vial, reaction will start)
10. Using a disposable spatula, stir in same direction for 5 min. under fume hood
11. Pour the slurry from Step 10 onto the PDMS mold slowly (*Note*: Take care to not allow the alumina to separate from polymer mixture)
12. Pack the slurry down into the sides of the mold with a toothpick or a plastic fork
13. Examine the bottom and sides of the mold to verify that there are no visible air pockets
14. Place PDMS mold inside the vacuum desicator. Vacuum for 10 minutes, then 10 minutes atmospheric release. Repeat cycle 4 times.
15. Remove PDMS mold from desicator and stir alumina slurry with a toothpick to re-mix the polymer and ceramic, re-pack slurry into the sides of the mold. Gently scrape over the top of the PDMS mold back and forth to break any residual bubble and/or to remove air pockets from the top surface of the PDMS. Examine the bottom and sides of the mold to verify that there are no visible air pockets
16. Repeat Steps 14 and 15 three times (*Note*: This is important as air pockets will burst during the furnace anneal and cause the device to shatter.)
17. Set mold aside and let air dry for 24 hours
18. Push down on top surface and pack alumina down into the mold. As the water evaporates the alumina needs to be constantly repacked to prevent holes/trapped air from forming in the mold. As the alumina dries the top surface will level out as the outside will sink into the sides of the mold

19. Repeat Step 18 every 12 hours for 7 days or till mold is hard to physical touch (*Note*: With air drying, it should take no longer than 10 days).
20. Place PDMS mold on hot plate at 50°C for 24 hours
21. Place PDMS mold on hot plate at 85°C for 24 hours
22. Place PDMS mold on hot plate at 150°C for 6 hours
23. Peel cured alumina out of PDMS mold

(Prakash)

APPENDIX B – SOLIDWORKS

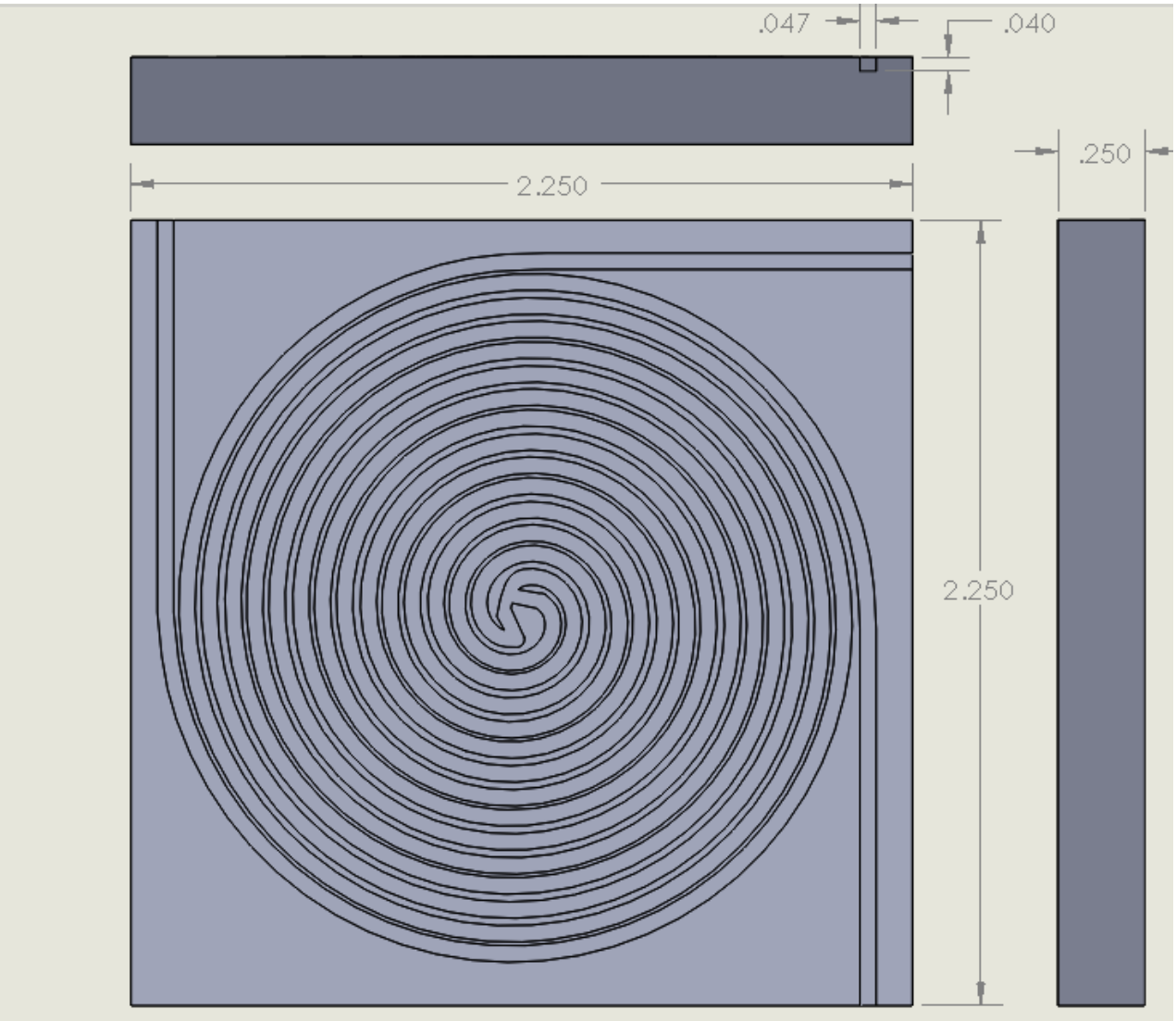

Figure 23: Geometry 1 of Microcombustor, Brass

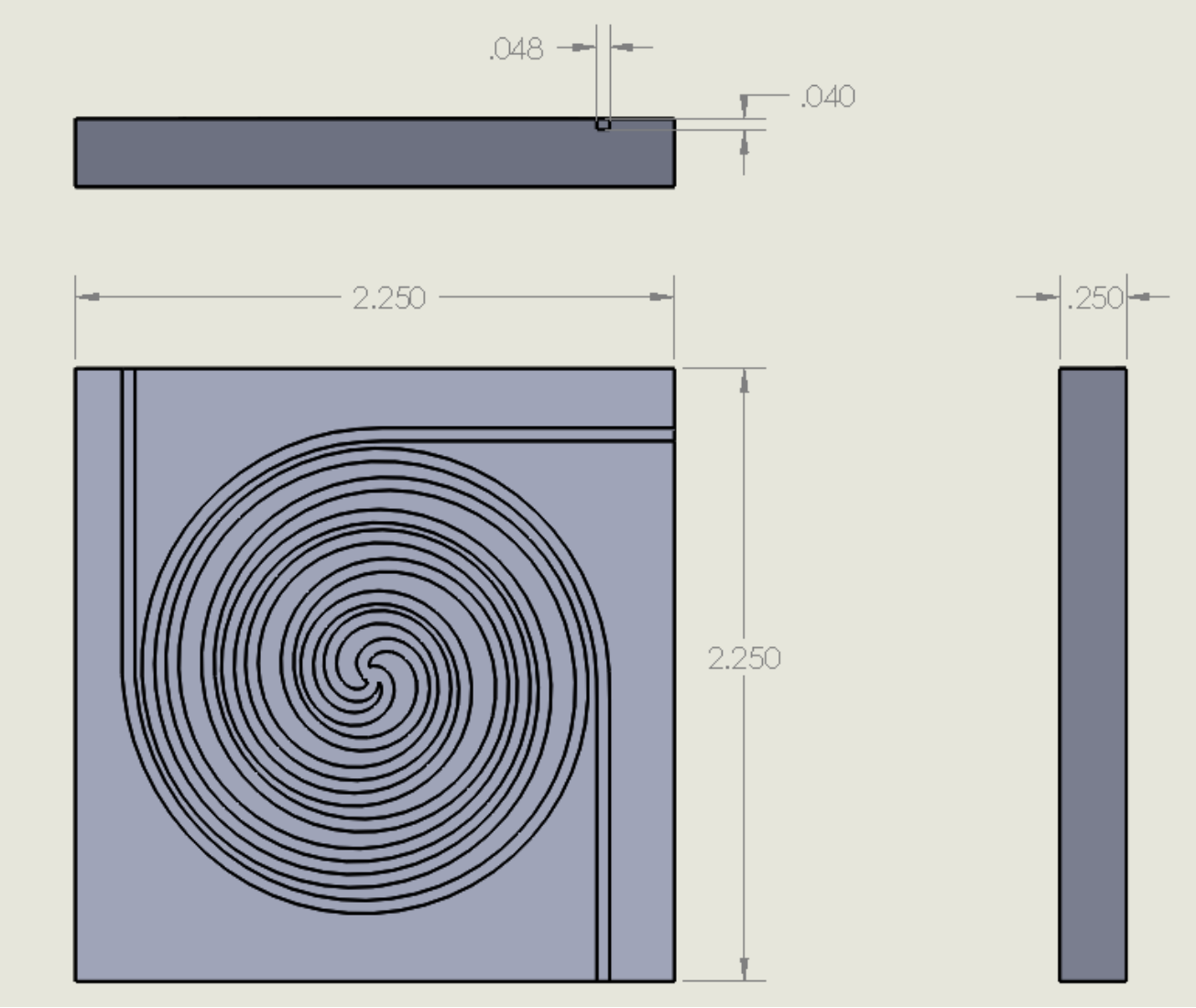

Figure 24: Geometry 2 of Microcombustor, Plastic from 3D Prototype Printing

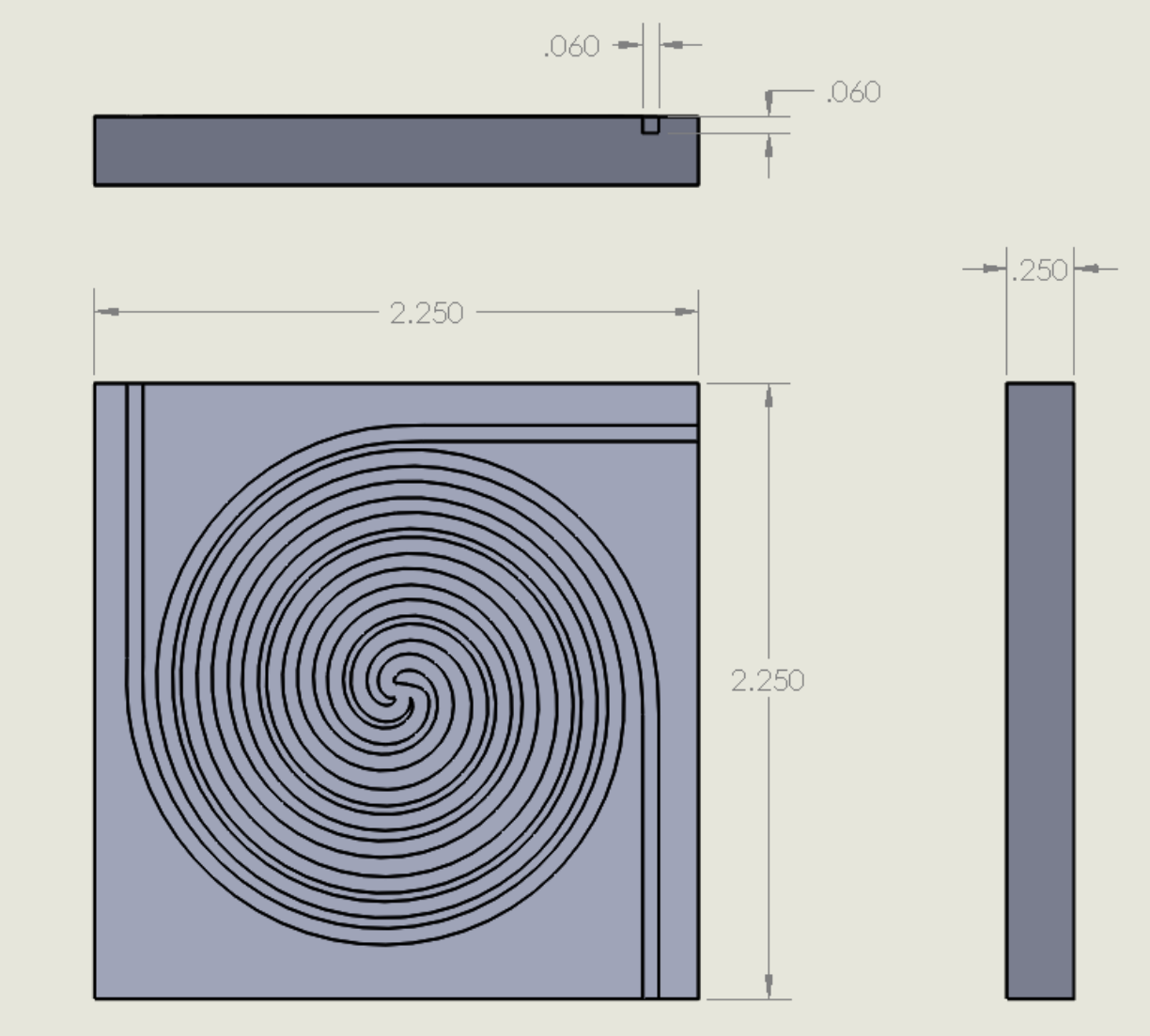

Figure 25: Geometry 3 of Microcombustor, Brass (Final)